Spin density and state of order in the alloy $Ni_{78}Mn_{22}$

G. Mazzone
Ente per le Nuove Tecnologie, l'Energia e l'Ambiente, Centro Ricerche Energia Casaccia, 00060 S. Maria di Galeria, Roma, Italy

C. Petrillo and F. Sacchetti
Dipartimento di Fisica, Università di Perugia, Via Pascoli, 06100 Perugia, Italy and Istituto di Struttura della Materia del Consiglio Nazionale delle Ricerche, Via Enrico Fermi 38, 00044 Frascati, Roma, Italy

M. Scafi
Dipartimento di Fiscia, Università di Roma "La Sapienza," Roma, Italy
(Received 26 May 1992)

The experimentally measured spin density of a partially ordered $Ni_{78}Mn_{22}$ alloy is used to study the magnetic state of Mn within an fcc environment. The present data, together with those obtained by Petrillo, Sacchetti, and Scafi [Phys. Rev. **44**, 9418 (1991)], are used to determine the form factor and magnetic moment of the Mn atoms in various atomic configurations. It is found that Mn carries a magnetic moment with fluctuating sign, while an appreciable charge transfer from Mn to Ni is suggested.

I. INTRODUCTION

In a previous paper,[1] we reported a neutron-diffraction investigation of the magnetic state of Mn in the fcc lattice of a partially ordered Ni-Mn alloy having atomic composition $Ni_{78}Mn_{22}$. The observation that Mn atoms are in a state of high magnetic moment, whose orientation is strongly affected by the local environment, warrants the study of the magnetic structure of this alloy at a higher degree of order. The aim of the present work is the description of the magnetic state of both Mn and Ni, using the minimum number of hypotheses needed to extract the magnetic-moment distribution at each lattice site. In particular, it will be shown that under a few simple hypotheses the neutron-diffraction data allow one to deduce the magnetic moment of both Mn and Ni as well as the corresponding form factors.

II. EXPERIMENT

The present experiment has been performed on the polarized-neutron diffractometer installed at the 1-MW Training, Research and Isotope Production Reactor of the Centro Ricerche Energia, Casaccia (Rome). A standard experimental setup was employed: a $Co_{0.92}Fe_{0.08}$ polarizing monochromator, neutron-spin reversal at 3 Hz, and 0.7-T vertical magnetic field at the sample, which was the same employed in the previous experiment.[1] Sample dimensions were $1\times1.8\times0.07$ cm^3, with the extended face parallel to the (100) plane. In order to have negligible half-wavelength contamination, a Ge(111) monochromator was employed at a wavelength of 1.104 Å.

The $L1_2$ unit cell contains two sets of sites (A and B) and, for whatever composition and/or degree of long-range order, gives rise to two types of reflections, fundamental and superlattice. The respective nuclear-structure factors $F_N^{\pm}(hkl)$ are the following:

fundamental: $F_N^{+}(hkl)=3b_A+b_B$

if h, k, and l have the same parity;

superlattice: $F_N^{-}(hkl)=b_A-b_B$ otherwise,

where b_l is the average nuclear-scattering length of the lth site. In our case it is convenient to define the long-range-order parameter S as

$$S=\frac{F_N^{-}(hkl)}{b(\mathrm{Ni})-b(\mathrm{Mn})},$$

where $F_N^{-}(hkl)$ is the measured nuclear-structure factor of the sample and b(Ni) and b(Mn) are the nuclear-scattering lengths of Ni and Mn.

In order to obtain a degree of order higher than that obtained in the previous experiment with an annealing at 420 °C, the crystal was first heated under vacuum at 700 °C for 1 h and then annealed at 400 °C for a time (3000 h) long enough to reach an equilibrium state. The long-range-order parameter was calculated from the integrated intensities of the (100), (200), (300), and (400) reflections, thus avoiding an absolute measurement of the nuclear-structure factor of the superlattice reflections. The measured value $S=0.553(4)$, although much larger than that of the previous experiment, $S=0.259(2)$, is still far from the maximum value of S compatible with the present composition, namely, $S_{\max}=0.88$.

The main part of the experiment consisted in the determination of the flipping ratios of 15 fundamental and 13 superlattice reflections. Standard corrections for incomplete polarization of the incoming beam, flipping efficiency, and half-wavelength contamination were applied. The extinction correction was applied using the

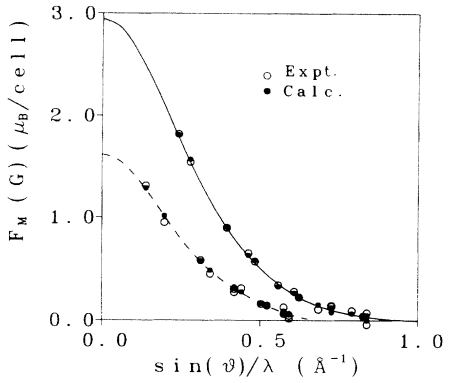

FIG. 1. Experimental structure factors (open circles) for fundamental (upper curve) and superlattice (lower curve) reflections. Also shown are the results of the fit described in the text (circles) and the spherical structure factors of fundamental (solid line) and superlattice (dashed line) reflections.

same parameters previously determined.[1] Bulk magnetization was measured on the same sample using a ballistic magnetometer.

Neutron-diffraction data were put on an absolute scale assuming $b(\mathrm{Mn})=-3.73$ fm and $b(\mathrm{Ni})=10.3$ fm for the nuclear-scattering amplitudes of Mn and Ni, respectively. The final magnetic-structure factors[2] are shown in Fig. 1, where the size of the circles represents the typical error.

III. RESULTS AND DISCUSSION

The present data have been analyzed together with those of Ref. 1 deriving for each site the average magnetic moment and average form factor by means of a well-established technique successfully employed in other cases.[1,3,4] For each site l, the following relations hold for the magnetic moment μ_l and spherical form factor $f_l(Q)$:

$$\mu_l=\frac{1}{\Omega_0}\sum_{\mathbf{G}} F_{\mathbf{G}}\int_{\mathrm{WS}(l)}\exp(i\mathbf{G}\cdot\mathbf{r})d\mathbf{r}\ , \tag{1a}$$

$$f_l(Q)=\frac{1}{\Omega_0\mu_l}\sum_{\mathbf{G}} F_{\mathbf{G}}\int_{\mathrm{WS}(l)} j_0(Qr)\exp(i\mathbf{G}\cdot\mathbf{r})d\mathbf{r}\ , \tag{1b}$$

where $\mathbf{G}$ is a reciprocal-lattice vector, Q is the modulus of the momentum transfer, Ω_0 is the unit-cell volume, and the integral is over the Wigner-Seitz cell WS(l) centered around the lth site. The results obtained from Eqs. (1a) and (1b) for the present state of order, together with those derived in the same way in Ref. 1, have been analyzed in a purely empirical fashion as described in what follows. Assuming that the spherical form factors of Ni and Mn and the magnetic moment of Ni are independent of the state of order as well as of the site, while the magnetic moment of Mn is left site and state of order dependent, the following relation is obtained for each value of Q:

$$(\mu_l f_l)^{\alpha}=p_l^{\alpha}(\mathrm{Mn})f(\mathrm{Mn})\mu_l^{\alpha}(\mathrm{Mn})+p_l^{\alpha}(\mathrm{Ni})f(\mathrm{Ni})\mu(\mathrm{Ni})\ , \tag{2}$$

where α refers to either the previous or present state of order, $p_l^{\alpha}(X)$, which can be deduced from the value of $S^{(1)}$, is the probability of finding the atom X at site l, and $f(\mathrm{Mn})$, $f(\mathrm{Ni})$, $\mu_l^{\alpha}(\mathrm{Mn})$, and $\mu(\mathrm{Ni})$ are the spherical form factors and magnetic moments of Mn and Ni. Since there are two states of order and two sites, Eq. (2) gives, at each Q, four relations containing two unknown form factors and five unknown magnetic moments, one for Ni and four for Mn. However, thanks to the fact that all form factors are equal to 1 at zero-momentum transfer, we can deduce $f(\mathrm{Mn})$ from Eq. (2) with no further assumptions. In fact, taking the difference

$$\Delta(Q)=\frac{[\mu_1 f_1(Q)]^{\alpha}}{p_1^{\alpha}(\mathrm{Ni})}-\frac{[\mu_2 f_2(Q)]^{\alpha}}{p_2^{\alpha}(\mathrm{Ni})}\ , \tag{3a}$$

where the subscripts 1 and 2 refer to the two sites, one has that the spherical form factor of Mn at each Q is given by the relation

$$f(\mathrm{Mn})=\frac{\Delta(Q)}{\Delta(0)}\ . \tag{3b}$$

From Eqs. (3), $f(\mathrm{Mn})$ can be determined independently for the two states α and α', thus allowing for a check of internal consistency. The Mn form factors obtained from the two sets of data compare quite well, and the average is shown in Fig. 2(a), together with $f(\mathrm{Mn})$ obtained using the structure factors of $MnPt_3$ as reported in Ref. 5. The

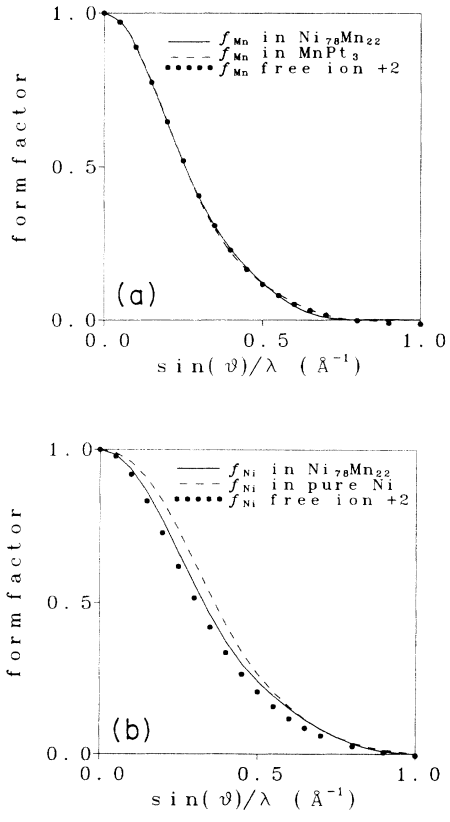

FIG. 2. (a) Form factor of Mn as deduced in the present system and in $MnPt_3$. For comparison, the free Mn^{2+} ion form factor is also reported. (b) Form factor of Ni as deduced in the present system and in pure Ni. The free ion Ni^{2+} form factor is also reported.

TABLE I. Magnetic moments of Mn and Ni deduced from the fit to the form factor (see text). The data refer to the present system (high S) and to the system studied in Ref. 1 (low S). The average magnetic moment for the Ni atom is also given.

Atom	Mn		Ni	
Site	Mn	Ni	Mn	Ni
Low S	1.122	0.11	0.247	0.191
High S	2.836	−0.80	0.364	0.420
Error	±0.020	±0.20	±0.070	±0.070
Average			0.306±0.050	

two results are in excellent agreement among themselves and with both the Mn form factor in $MnPt_3$ (Ref. 5) and with the form factor calculated[6] for the free Mn^{2+} ion, also shown in Fig. 2(a). In order to proceed further, one needs some information derived from other measurements. In particular, if a good estimate for f(Ni) was available, from a fit to the measured values of $(\mu_l f_l)^\alpha$ it would be possible to deduce the two magnetic moments appearing in Eq. (2), owing to the fact that the form factors of Mn and Ni differ appreciably. The simplest choice is the use of the form factor of pure Ni measured by Mook,[7] which, however, gives a rather poor fit. However, this fit shows clearly that the Ni form factor in the present alloy is more contracted than in the pure metal, while its magnetic moment is smaller. This behavior, namely, a more contracted form factor and smaller magnetic moment, has been already observed in disordered Ni-Cu alloys.[8] Therefore we have fitted $(\mu_l f_l)^\alpha$, employing the spherical form factor deduced from the data of Ref. 8, using Eq. (1b). The fit obtained in this way allows us to perform a check of internal consistency comparing the magnetic moments of Ni deduced from the four determinations of $(\mu_l f_l)^\alpha$. The magnetic moments so derived are reported in Table I, which shows that these moments are appreciably lower than that of pure Ni metal. This result is in agreement with a number of other experimental observations on the Ni-Mn system.[9] In order to improve the self-consistency of our data, we have averaged the Ni moments and recalculated the Ni form factor for each set of data. These form factors are very similar to each other and also to the form factor of Ref. 8, which was the starting point of this procedure, so that their average is fairly well representative of the Ni form factor in the present alloy. This average value of the Ni form factor is shown in Fig. 2(b) compared with that of the pure metal and that calculated[6] for the free Ni^{2+} ion. As one can see, there is an appreciable difference between pure Ni and Ni in the present alloy. Moreover, this difference is much more pronounced than the fluctuations among the individual determinations of the Ni form factor in the present alloy. Therefore we can conclude that in $Ni_{78}Mn_{22}$ the spin distribution of Mn is very close to

TABLE II. Parameters of the fit to the experimental structure factors as described in the text.

μ_{Mn}	μ^a_{Mn}	μ_{Ni}	μ^a_{Ni}
1.948±0.009	0.05±0.10	0.332±0.003	−0.140±0.043

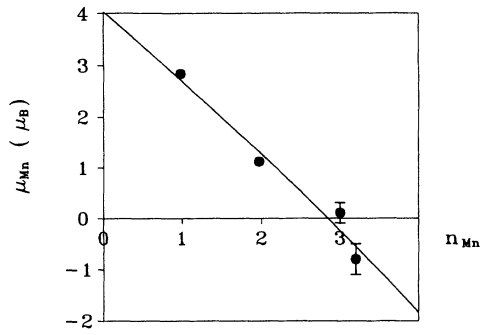

FIG. 3. Mn magnetic moment as a function of the average number of Mn atoms in the first shell. The solid line is a guide for the eye.

that of the free Mn^{2+} ion, while that of Ni shows a remarkable trend, probably due to the change of the paired-electron contribution. This trend can be appreciated looking at the Ni^{2+} form factor[6] obtained from a restricted calculation (that is, such that there is no dependence of the $3d$ wave function on the spin state), which is the limiting case of no contribution of the paired electrons.

Further information about the electronic distribution can be obtained from the asphericity of the spin density. We start writing the structure factor in the form

$$F_G = \sum_l \cos(\mathbf{G}\cdot\mathbf{R}_l)[\mu_l f_l(G)+\mu_l^a f_l^a(\mathbf{G})] , \tag{4}$$

where $\mathbf{R}_l$ is the position of the lth site in the unit cell, μ_l and $f_l(G)$ are the magnetic moment and spherical form factor given in Eqs. (1a) and (1b), and μ_l^a and $f_l^a(\mathbf{G})$ are the aspherical magnetic moment and form factor. Taking into account the irreducible representations Γ_{12} and $\Gamma_{25'}$, the aspherical form factor is given by[1]

$$f_l^a(\mathbf{G}) = A(\mathbf{G}) f_l^{(4)}(G) , \tag{5a}$$

$$f_l^{(4)}(G) = \frac{1}{\Omega_0 \mu_l} \sum_{\mathbf{G}} \int_{WS(l)} j_4(Qr)\exp(i\mathbf{G}\cdot\mathbf{r})d\mathbf{r} , \tag{5b}$$

where $A(\mathbf{G})$ is the appropriate angular factor.[4] In Eq. (4), μ_l and μ_l^a have been treated as free parameters. Note

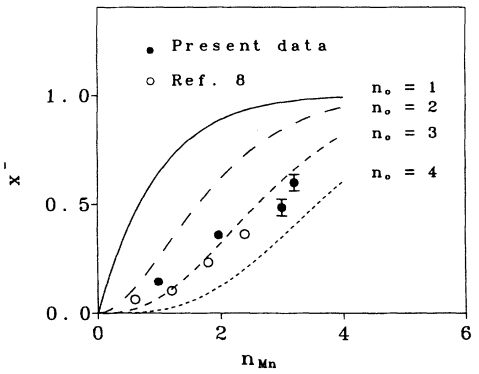

FIG. 4. Percentage of magnetic moment reversal x^- (see text) as a function of the number of Mn atoms first nearest neighbors.

TABLE III. Aspherical magnetic moments of Mn and Ni in the present high-order system and in the low-S system of Ref. 1. The value of pure Ni is also reported.

Atom	Mn	Ni
Low S	0.14±0.30	−0.174±0.060
High S	0.23±0.20	−0.148±0.040
Pure metal		−0.314±0.030

that although one could use for μ_l the values derived from Eq. (1a), we have chosen to leave it as a free parameter in order to reduce the possible influence of systematic errors on μ_l^a. The results of the fit are reported in Table II. The analysis of the data of Tables I and II can be performed assuming a fixed value of the magnetic moment for both atoms and leaving the possibility of a spin reversal of Mn, when the number of Mn nearest neighbors exceeds a certain number n_0, as done in Ref. 1. This is actually the simplest model which, if applied to the present coherent-scattering data, may provide some information on the modulus of the Mn magnetic moment. As shown in Fig. 3, there is an essentially linear relation between the average Mn magnetic moment and average number of Mn nearest neighbors n_{Mn}. Of course, with the present alloy, there is no direct way to deduce the Mn magnetic moment when an atom of Mn has no other Mn nearest neighbors. Furthermore, there is no reason for a functional dependence of the Mn magnetic moment on the configuration of the first shell only. On the contrary, there is an indication that in disordered alloys[9] the magnetic interaction among Mn atoms extends beyond the first shell. Nevertheless, the hypothesis that the modulus of the Mn magnetic moment has a value of about $4\mu_B$ is strongly suggested by Fig. 3 and appears quite reasonable considering the results of other experiments.[1,5,10,11]

Once the modulus $\mu^0(\mathrm{Mn})=4\mu_B$ is determined, one can use a spin-reversal probability x^-, such that

$$\mu(\mathrm{Mn})=\mu^0(\mathrm{Mn})(1-2x^-)\ , \tag{6}$$

where x^- depends on the site and is also a function of both S and the composition of the alloy. Equation (6) allows one to calculate x^-, which is shown in Fig. 4 as a function of n_{Mn} and in comparison with a simple random model defined by a binomial distribution

$$x^-=\sum_{n_0^n}^{12}\begin{bmatrix}12\\ n\end{bmatrix}\left[\frac{n_{\mathrm{Mn}}}{12}\right]^n\left[\frac{1-n_{\mathrm{Mn}}}{12}\right]^{12-n}\ , \tag{7}$$

which corresponds to the assumption that $\mu(\mathrm{Mn})$ is reversed with respect to the matrix magnetization when n_{Mn} is greater than or equal to a reference number n_0. As we can see, the $n_0=3$ curve fits reasonably the present experimental data, as well as those reported in Ref. 9 for disordered alloys and interpreted using Eq. (6). The observed behavior shows that the spin-reversal mechanism has a definite meaning, at least at an average level, in the sense that the distribution of $\mu(\mathrm{Mn})$ contains two main peaks centered at $-4\mu_B$ and $+4\mu_B$, having weights $(1-x^-)$ and x^-. Accordingly, we can analyze also the aspherical magnetic moments reported in Table II, assuming that the aspherical magnetic moment of Ni is independent of both state of order and site and that Eq. (6) holds also for $\mu^a(\mathrm{Mn})$ with the same value of x^- as determined for the total magnetic moment. The atomic aspherical magnetic moments thus obtained are reported in Table III, where we see that Ni in this alloy has the same symmetry of the pure metal since $\mu^a(\mathrm{Ni})/\mu(\mathrm{Ni})$ has the same value in both cases.

TABLE IV. Occupation numbers of various electron states as obtained from the present experiment (see text).

Atom	Mn	Ni
$n_{\Gamma_{12\uparrow}}$	2.00	2.00
$n_{\Gamma_{25'\uparrow}}$	3.00	3.00
$n_{\Gamma_{12\downarrow}}$	0.32	1.94
$n_{\Gamma_{25'\downarrow}}$	0.68	2.76
$n_{s\uparrow+\downarrow}$	0.45	0.45
Charge transfer	−0.55	+0.15
γ_c	0.61	0.59

A further observation concerns the decrease of the Ni magnetic moment, which in our opinion is due mainly to charge transfer from Mn to the spin-down d band of Ni. In this connection it is very tempting to associate with this charge transfer the occurrence in the present alloy of a magnetic moment of Mn much higher than that calculated for pure fcc Mn,[12,13] at least for values of the lattice parameter close to those experimentally observed. Of course, this charge transfer cannot be demonstrated from the present data; however, it seems a plausible conjecture in view of the systematic decrease of the Ni magnetic moment in ferromagnetic Ni-Mn alloys as the Mn concentration is increased[9] and considering that the work function of Mn is considerably smaller than that of Ni. The above argument for Ni and the high value of the Mn magnetic moment lead to the conclusion that both Ni and Mn have the spin-up d band essentially full. If, as in the case of Fe-Co,[3] we add the simple hypothesis that the number of s-like electrons is the same on both atoms, because of the delocalized nature of the corresponding one-electron wave functions, we can derive reasonable values of the occupation numbers of all the electron states of the two atoms. These numbers together with the $\Gamma_{25'}$ percentage of the total charge distribution γ_c are reported in Table IV. With the help of Table IV, it is immediate to calculate the difference between the nuclear charge and number of electrons in each Wigner-Seitz cell, i.e., the charge transfer, which turns out to be appreciable for both atomic species. In conclusion, our analysis suggests that the magnetic state of Mn in this alloy, characterized by a very high magnetic moment, could be related to the occurrence of a significant amount of charge transfer, which, in any case, plays an important role in determining the occupation numbers of the various electron states. If this conclusion is true, one might expect that in situations with no appreciable charge transfer from Mn to the other atomic species, such as, for instance, in concentrated Mn alloys, the magnetic moment of Mn could have a value closer to that calculated for pure fcc Mn, as indeed observed in most transition-metal–manganese alloys.

[1]C. Petrillo, F. Sacchetti, and M. Scafi, Phys. Rev. B **44**, 9418 (1991).
[2]The experimental structure factors are available directly from the authors.
[3]E. Di Fabrizio, G. Mazzone, C. Petrillo, and F. Sacchetti, Phys. Rev. B **40**, 9502 (1989).
[4]F. Menzinger and F. Sacchetti, Nukleonika **24**, 737 (1979).
[5]F. Menzinger, F. Sacchetti, and M. Romanazzo, Phys. Rev. B **5**, 3778 (1972).
[6]*International Tables for X-ray Crystallography*, edited by J. A. Ibers and W. C. Hamilton (Kluwer Academic, Dordrecht, 1989), Vol. IV, p. 103.
[7]H. A. Mook, Phys. Rev. **148**, 495 (1966).
[8]F. Sacchetti, P. De Gasperis, and F. Menzinger, Phys. Status Solidi B **76**, 309 (1976).
[9]J. W. Cable and H. R. Child, Phys. Rev. B **10**, 4607 (1974).
[10]P. Bisanti, G. Mazzone, and F. Sacchetti, J. Phys. F **17**, 1425 (1987).
[11]J. W. Cable, E. O. Wollan, W. C. Koehler, and H. R. Child, Phys. Rev. **128**, 2118 (1962).
[12]N. A. Cade, J. Phys. F **11**, 2399 (1981).
[13]G. Fuster, N. E. Brener, J. Callaway, J. L. Fry, Y. Z. Zhao, and D. A. Papaconstantopoulos, Phys. Rev. B **38**, 423 (1988).